Redox Biology 24 (2019) 101166

Contents lists available at ScienceDirect

Redox Biology

journal homepage: www.elsevier.com/locate/redox

Research Paper

The vitamin E derivative garcinoic acid from *Garcinia kola* nut seeds attenuates the inflammatory response

Maria Wallert[a,b,c,1], Julia Bauer[c,d,1], Stefan Kluge[b,c], Lisa Schmölz[b,c], Yung-Chih Chen[a], Melanie Ziegler[a], Amy K. Searle[a], Alexander Maxones[e], Martin Schubert[b,c], Maria Thürmer[f], Helmut Pein[f], Andreas Koeberle[f], Oliver Werz[b,f], Marc Birringer[e], Karlheinz Peter[a,g,1], Stefan Lorkowski[b,c,*,1]

[a] *Atherothrombosis and Vascular Biology Laboratory, Baker Heart and Diabetes Institute, Melbourne, Victoria, Australia*
[b] *Competence Cluster of Nutrition and Cardiovascular Health (nutriCARD), Jena-Halle-Leipzig, Germany*
[c] *Department of Nutritional Biochemistry and Physiology, Institute of Nutrition, Friedrich Schiller University Jena, Jena, Germany*
[d] *Institute of Human Genetics, University Medical Center Goettingen, Göttingen, Germany*
[e] *Department of Nutritional, Food and Consumer Science, University of Applied Sciences Fulda, Fulda, Germany*
[f] *Department of Pharmaceutical/Medicinal Chemistry, Institute of Pharmacy, Friedrich Schiller University Jena, Jena, Germany*
[g] *Central Clinical School, Monash University, Melbourne, Australia*

ARTICLE INFO

Keywords:
Garcinoic acid
Garcinia kola seeds
Inflammatory response
Macrophage activation
Atherosclerosis

ABSTRACT

The plant *Garcinia kola* is used in African ethno-medicine to treat various oxidation- and inflammation-related diseases but its bioactive compounds are not well characterized. Garcinoic acid (GA) is one of the few phytochemicals that have been isolated from *Garcinia kola*.

We investigated the anti-inflammatory potential of the methanol extract of *Garcinia* kola seeds (NE) and purified GA, as a major phytochemical in these seeds, in lipopolysaccharide (LPS)-activated mouse RAW264.7 macrophages and its anti-atherosclerotic potential in high fat diet fed ApoE$^{-/-}$ mice.

This study outlines an optimized procedure for the extraction and purification of GA from *Garcinia kola* seeds with an increased yield and a purity of > 99%. We found that LPS-induced upregulation of iNos and Cox2 expression, and the formation of the respective signaling molecules nitric oxide and prostanoids, were significantly diminished by both the NE and GA. In addition, GA treatment in mice decreased intra-plaque inflammation by attenuating nitrotyrosinylation. Further, modulation of lymphocyte sub-populations in blood and spleen have been detected, showing immune regulative properties of GA.

Our study provides molecular insights into the anti-inflammatory activities of *Garcinia* kola and reveals GA as promising natural lead for the development of multi-target drugs to treat inflammation-driven diseases.

1. Introduction

Natural products obtained from plants are widely used in folk medicine. The number of novel natural products described every year is large and systematic efforts are needed to elucidate their effectiveness and functions as bioactive principles or lead structures for drug development. A good example for the use of extracts in phytomedicine is the African plant *Garcinia kola* [1], which was first described for its antimicrobial properties by Hussain et al., in 1982 [2]. Until today several additional effects, such as radical scavenging [3], anti-oxidative [4] and anti-inflammatory properties [5], have been reported. Since this plant contains several bioactive compounds, namely garcinoic acid (GA) [6], it represents an interesting source to study putative pharmacological actions [7].

Our compound of interest, GA, also known as *trans*-13′-carboxy-δ-tocotrienol, contains an oxidative modification at its side chain and is a principle hepatic metabolite of dietary δ-tocotrienol (T3) [6]. In addition to tocopherols (TOH), T3s represent a less abundant form of vitamin E. TOHs and T3s, which differ in the saturation of the side chain, are further divided into α-, β-, γ- and δ-forms showing specific methylation patterns of the chromanol ring. However, in the last decades T3s have been described to potently interfere with inflammation and

* Corresponding author. Institute of Nutrition, Friedrich Schiller University Jena, Dornburger Str. 25, 07743 Jena, Germany.
E-mail address: stefan.lorkowski@uni-jena.de (S. Lorkowski).
[1] These authors contributed equally.

https://doi.org/10.1016/j.redox.2019.101166
Received 7 February 2019; Received in revised form 4 March 2019; Accepted 10 March 2019
Available online 12 March 2019

oxidative stress *in vitro* [8,9] and in animal models [10,11]. In addition, T3s affect macrophage recruitment [12] – a key event in atherosclerosis. In line with this data, anti-atherosclerotic effects of T3s have been shown in ApoE$^{-/-}$ mice by Shibata and colleagues [13].

Recent studies demonstrated that carboxylation of the side chain significantly increases the anti-inflammatory capacity of TOHs [14–16]. Similar effects have been demonstrated for GA, an oxidized δ-T3, which inhibits mPGES-1 *in vitro* [17]. Therefore, we investigated the anti-inflammatory effects of GA in comparison to the methanol extract of *Garcinia kola* seeds (NE) in LPS-activated RAW264.7 macrophages to elucidate the contribution of the latter phytochemical. Further, we studied the effectiveness of GA in decreasing inflammation-related formation of atherosclerotic plaques using an atherosclerotic mouse model to estimate the potential of GA as a promising new therapeutic lead molecule against inflammation-driven diseases.

2. Materials and Methods

2.1. Chemicals

If not indicated otherwise, chemicals were obtained from Carl Roth (Karlsruhe, Germany), Sigma-Aldrich (Seelze, Germany), or Merck Millipore (Darmstadt, Germany).

2.2. Extraction of Garcinia kola seeds and isolation of GA

2.2.1. Standard preparation of NE

The standard preparation of the NE was performed according to published procedures [4,18,19] (Suppl. Fig. S1).

2.2.2. Optimized preparation of NE

NE from *Garcinia kola* seeds was obtained using Bligh and Dyer extraction [20]. Thus, 100 g crushed seeds and methanol/chloroform (400 ml/800 ml) were shaken for 4 h. After filtering, 400 ml of a 2% (w/v) NaCl solution was added and the mixture was shaken vigorously for 5 min. The chloroform phase was dried using Na_2SO_4 and the solvent was evaporated (Suppl. Fig. S1).

2.2.3. Isolation and purification of GA

Purification of GA was performed as reported with slight modifications [4,18,19]. In brief, seed extract was dissolved in methanol/chloroform (95%/5%, v/v) and applied to a silica gel column to isolate a crude product. Presence of GA in collected eluates was tested using thin-layer chromatography with dichloromethane/methanol (95%/5%, v/v) as solvent. Subsequently, re-chromatography of GA-containing aliquots was performed on a silica gel using a hexane/acetone (65%/35%, v/v) mixture. GA was characterized by high-performance liquid chromatography coupled with mass spectrometry (Fig. 1 and flow chart in Suppl. Fig. S1).

2.2.4. Liquid chromatography coupled with tandem MS (LC-MS/MS) analysis

The LC-MS/MS system consisted of a Dionex UltiMate 3000 UHPLC system coupled to a Bruker AmaZon SL Ion trap mass spectrometer equipped with an atmospheric pressure chemical ionisation (APCI) source (Bruker, Karlsruhe, Germany). The chromatography utilized a Kinetex F5 Core-Shell column (2.1 × 100 mm, 2.6 µm) from Phenomenex (Aschaffenburg, Germany) connected to a SecurityGuard ULTRA cartridge (Phenomenex). The solvent system consisted of methanol/formic acid (1000:1 v/v, A) and H_2O/formic acid (1000:1 v/v, B). The separation was performed with a multi-step gradient scheme as follows: 0 min, 70% B; 3 min, 70% B; 5 min, 80% B; 10 min 80% B; 12 min, 90% B; 18 min, 90% B; 20 min, 100% B (flow rate 0.2 ml/min). Data were analyzed using basic peak monitoring and negative polarity APCI (dry gas temperature: 250 °C, flow: 4.2 l/min; nebulizer pressure: 34.8 psi; vaporizer temperature: 380 °C; capillary voltage: 4000 V; end plate offset: 500 V) with Bruker Compass Data Analysis software version 4.2.

2.3. RAW264.7 macrophage culture

Murine RAW264.7 macrophages (ATCC, Manassas, VA) were cultivated as described previously [16]. For experiments, cells were incubated as indicated in the figure legends and harvested for further processing as described below. For detailed information, see the Suppl. Materials and Methods section.

2.4. Animal experiments and treatment

All animal procedures were approved by the Animal Ethics Committee of the Alfred Medical Research and Education Precinct (AMREP), Melbourne, Australia (Ethic number E/1658/2016/B) and was performed in accordance with the Australian code for care. To investigate the effect of GA on the progression of atherosclerosis, eight weeks old male apolipoprotein E knockout (ApoE$^{-/-}$) mice (C57Bl/6 background, 25–28 g), ad libitum fed a HFD (22% fat and 0.15% cholesterol, SF00-219, Specialty Feeds, Western Australia, Suppl. Table S1) for further eight weeks, have been used. Mice were randomly assigned to receive 1 mg/kg body weight of GA (n = 9) or vehicle (PBS + 0.8% DMSO, n = 9) via intraperitoneal (IP) injection weekly. At the age of 16 weeks, mice have been anesthetized using ketamine (50 mg/kg, Parnell Laboratories, NSW, Australia) and xylazine (10 mg/kg, Troy Laboratories, NSW, Australia). Blood and tissue samples were collected and processed as described below. Grouping of animals and quantifications were blinded from the responsible researchers throughout the study.

2.5. RNA isolation, cDNA synthesis and quantitative real-time PCR (RT-qPCR)

Total RNA isolation (Qiagen, Hilden, Germany), cDNA synthesis (Fermentas, St. Leon-Rot, Germany) and RT-qPCR analysis (LightCycler 480 II instrument, Roche Diagnostics, Mannheim, Germany) have been performed as described previously [16]. Primers (Suppl. Table S2) were purchased from Invitrogen (Karlsruhe, Germany).

2.6. Immunoblotting

Cell harvesting, sample preparation and antibody usage are according to Wallert et al. [16] For the detection of α-tubulin (55 kDa), Cox2 (72 kDa) and iNOS (130 kDa), PageRuler™ Prestained Protein Ladder (10–180 kDa) from Thermo Fisher Scientific (Schwerte, Germany) was used.

2.7. Quantification of nitric oxide (NO) formation using Griess assay

Griess assay was used to measure nitrite in the supernatant of RAW264.7 macrophages (Enzo Life Science) and in murine plasma samples (Promega). Macrophages were incubated with either solvent (DMSO), 1.25 µg/ml NE or 2.5 µM GA in serum free high glucose DMEM for 4 h followed by a combined incubation with 100 ng/ml LPS for 20 h. For Griess assay, collected cell supernatants were prepared as outlined in Wallert et al. [16]. Murine plasma samples were prepared according to manufacturer's protocol. Absorbance was measured at 540 nm using a Fluostar omega plate reader (BMG Labtech, Offenbach, Germany and Adelaide, Australia).

2.8. Quantification of prostanoids using reversed phase UPLC-MS/MS and ELISA

Thromboxane (Tx)B_2 release from RAW264.7 macrophages was measured using an ELISA Kit from Enzo life Sciences (Lörrach, Germany) according to the manufacturer's protocol. In addition,

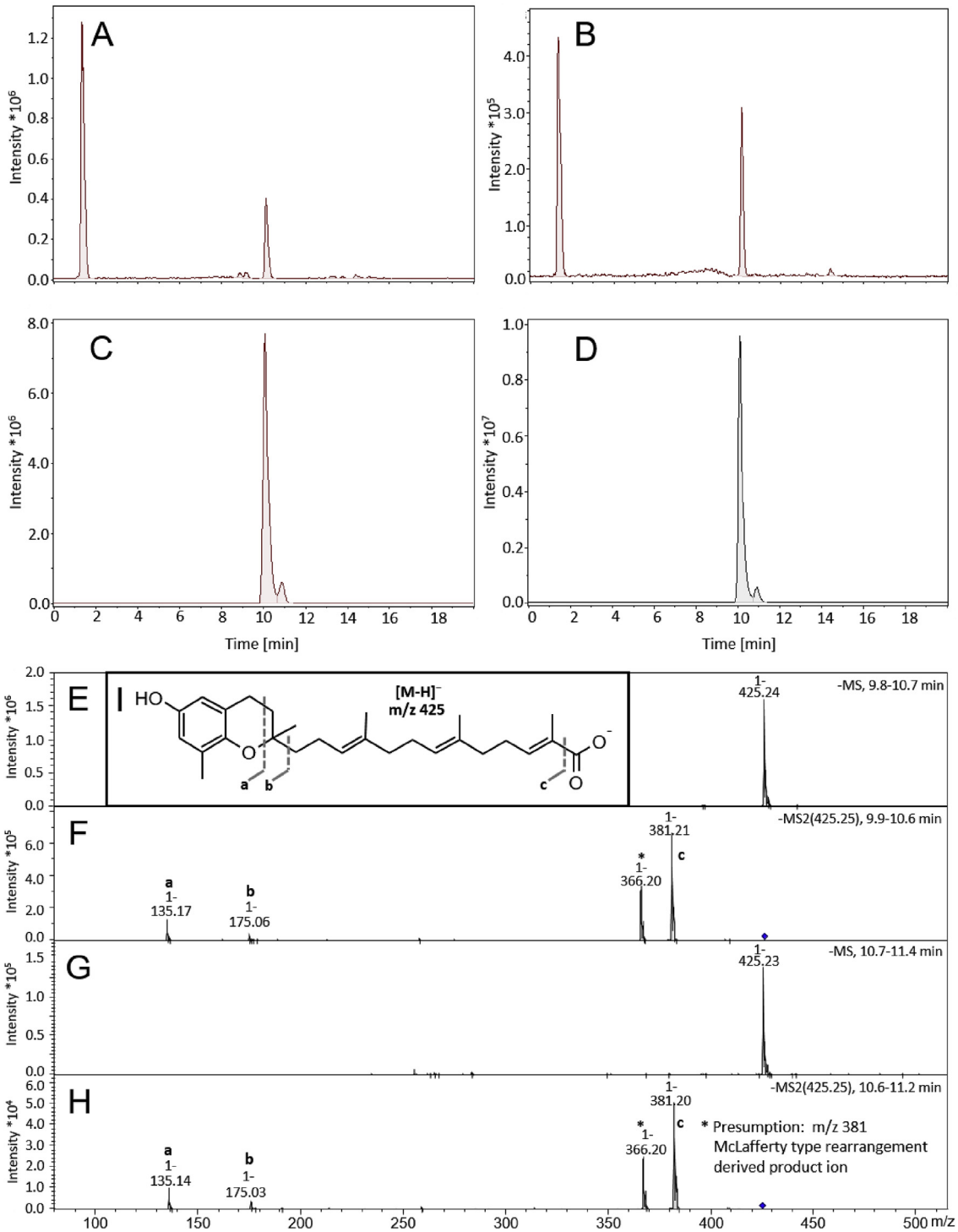

Fig. 1. Bligh and Dyer extraction increased the yield of garcinoic acid (GA) isolated from *Garcinia kola* seeds at high purity. Representative LC-MS chromatograms of the *Garcinia kola* seeds extracts obtained by the standard procedure **(A)** and by Bligh and Dyer extraction **(B)**. Panel **(C)** and **(D)** show LC-MS chromatograms of the purified GA obtained from crude methanol extract from *Garcinia kola* seeds according to the procedures used for **(A)** and **(B)**, respectively. Mass spectra of the purified GA were obtained from the LC-MS chromatogram **(D)** for two peaks with retention times of 9.8–10.6 min (main peak, **E**) and 10.7–11.4 min (minor peak, **G**). MS/MS fragmentation spectra of **(E)** and **(G)** are shown in panels **(F)** and **(H)**. The fragmentation is indicated on structure **(I)**, respectively.

prostaglandins and TxB_2 were extracted from RAW264.7 cell supernatants and murine plasma, separated on an Acquity UPLC BEH C18 column (1.7 µm, 2.1 × 50 mm; Waters, Milford, MA) using an Acquity™ UPLC system (Waters), and detected using a QTRAP 5500 MS (Sciex, Darmstadt, Germany) equipped with an electrospray ionisation source as previously described [16].

2.9. Histology and immunohistochemistry

For histology and immunohistology transversal cryosections of O.C.T. embedded aortic sinus (6 µm) were prepared (Zeiss MICROM HM 550). For detailed information see Suppl. Materials and Methods section.

2.9.1. Histological staining

For H&E staining, fixed sections (70% EtOH, 10% formalin, 5% glacial acetic acid, 15% dH_2O, 5 min) were washed twice in 70% EtOH (30 s) and dH_2O (5 min) and stained with Mayer's Hematoxylin (2 min), followed by Puff's Eosin solution (20 s), dehydrated and cleaned using 100% EtOH and Xylene, respectively. Finally, samples were mounted with Depex to ensure their longevity. To stain collagen content, samples were fixed in 10% formalin for 20 min and placed in 0.1% PSR (0.5 g Sirius Red in 500 ml Picric Acid Solution) solution for 1 h. After differentiation with 0.01 M HCl, samples were washed, dehydrated, cleaned and mounted as described above. Lipid content was determined using isopropanol/dH_2O diluted (3:2 v/v) and filtered ORO. Samples were fixed (10% formalin, 4 min) and washed in 60% isopropanol (25 s) before staining with ORO (1 h), differentiated in 60% isopropanol, washed, counterstained with Mayer's hematoxylin (45 s) and mounted in Aquatex (Merck Millipore, Bayswater, VIC, Australia).

2.9.2. Immunohistochemical staining

Quantification of plaque stability, intra-plaque inflammation and cell infiltration was determined using antibodies against nitrotyrosine, Interleukin (IL)1β, vascular cell adhesion protein (VCAM)-1, monocyte chemoattractant protein (MCP)-1 and the macrophage marker CD68. Fixed sections were washed with PBS, blocked with 3% hydrogen peroxide, washed with PBS supplemented with 0.05% Tween20 and blocked with 10% horse or rabbit serum according to host of antibody species. After Avidin and Biotin blocking (Vector Laboratories, Burlingame, CA, USA), except for IL1β and MCP-1 staining, primary antibodies, diluted in blocking solution, were applied. Afterwards, washed samples were incubated with the respective secondary antibody diluted in blocking solution for 30 min, followed by conversion of the chromophoric horseradish peroxidase substrate diaminobenzidine (Vector Laboratories). Finally, samples were counterstained, dehydrated with 95% EtOH followed by 100% EtOH (twice), cleaned using Xylene (twice) and mounted with Depex. Respective IgG and omit antibody controls have been performed (Suppl. Fig. S2). Positive stained area of four sections per sample were analyzed using OPTIMAS version 6.2 VideoPro-32 system.

2.10. Flow cytometer analysis to investigate immunologic cell pattern

Antibodies were purchased from BD Bioscience if not otherwise indicated. Blood was collected in 0.5 M anti-coagulant ethylenediaminetetraacetic acid (EDTA) using cardiac puncture. Spleen was removed and stored on ice (PBS, 2 mM EDTA, 0.1% bovine serum albumin, BSA). Within 1 h of collection, cells from blood and spleen have been isolated, red blood cells were lysed (BD FACS lysing solution), and remaining cells were filtered and plated for further staining. Total monocyte/macrophage population was detected using CD11b-FITC and CD115-PE-Cy7 antibodies (Biolegend, San Diego, CA, USA). In addition, Ly6C-PB staining was performed to separate pro- and anti-inflammatory monocytes sub-populations. B cell lymphocytes have been gated using CD19-PE (BD Bioscience) staining. T cell lymphocytes were categorized in CD4 (PB) and CD8 (PerCP) positive cells as well as natural killer T (NKT) cells via NK1.1-PE-Cy7 and T-cell receptor β (TCR-β) staining. NK1.1-PE-Cy7 positive and TCR-β negative cells were gated as natural killer (NK) cells (Suppl. Fig. S3). Cell populations were analyzed using flow cytometry (FACSCanto II, BD Biosciences, USA) and analyzed with BD FACS DIVA software version 8.0.1.

2.11. Lipid measurement

Blood samples were taken as described above and centrifuged (300 × *g*, 10 min, room temperature) to separate plasma within 1 h of collection. Total serum cholesterol, LDL, HDL and triglycerides were measured using COBAS Integra 400 Plus blood chemistry analyzer (Roche Diagnostics, Australia).

2.12. Statistics

Data are presented either as means ± standard deviation (SD) or as means ± standard error of the mean (SEM) of independent experiments. In order to test for statistical significance, paired Student's t-tests was performed using Microsoft Excel 2010. ANOVA followed by Tukey post-hoc tests with logarithmized values and one-way ANOVA with multiple comparisons were used as outlined in the respective figure legends.

3. Results

In the here outlined study we pursued two aims. Firstly, the optimization of the extraction procedure of GA starting from *Garcinia kola* seeds to ensure the most effective use of these rare seeds. Secondly, the characterization of GA, as one of the main phytochemicals in *Garcinia kola* seeds, by focusing on anti-inflammatory effects and its potential as a drug for the treatment of inflammation-driven diseases.

3.1. Bligh and Dyer extraction increases the yield of GA

The extraction method of GA from *Garcinia kola* seeds firstly published by Terashima et al. [4] and slightly modified by Birringer et al. yields up to 0.38% GA[18]. The isolation of the GA follows in principle two steps: (i) the methanol extraction of the seed, and (ii) the purification of GA. Using our optimized approach, we were able to increase the quantity of NE 2.3-fold and the purified GA 6.6-fold (Suppl. Fig. S1) and were able to highly purify GA by silica gel chromatography (> 99%). Chromatographic separation revealed a major peak with *m/z* 425.4 $[M\text{-}H^+]^-$ at a retention time (RT) of 10.2 min representing GA and a minor peak at a RT of 10.8 min with identical mass. As the MS/MS spectra of the two peaks showed identical fragmentation patterns, we assume that the minor compound is a stereoisomer (either the *cis/trans* or the diastereomeric form) of GA (Fig. 1).

3.2. Purified GA blocks the LPS-induced expression of inflammatory mediators in murine macrophages

Previous studies demonstrated anti-inflammatory potential of a *Garcinia kola* seeds extract in rats [21]. One of the major compounds in this extract is GA, a T3 metabolite [18]. It has been shown that T3s are highly potent in blocking the inflammatory response of macrophages [8]. Therefore, we investigated the effects of both the NE and purified GA on LPS-induced inflammatory response in murine RAW264.7 macrophages. First, we analyzed the effect of GA on the expression of classic LPS-responsive genes such as Il6, Il1β, Tnfα, Cox2 and iNos, which encode pro-inflammatory mediators (Suppl. Table S2). Neither the NE nor GA affected basal expression levels of these marker genes (Fig. 2A–F, white bars). As expected, LPS significantly induced the expression of the genes of interest. The LPS response was efficiently blocked by both the NE and even stronger by GA as indicated in the figures (Fig. 2A–F, grey bars). Expression of Tnfα was significantly blocked to similar extent by different concentrations of GA (Fig. 2A, right column), whereas the NE tended to decrease Tnfα expression (Fig. 2A, left column). GA blocked the LPS-induced expression of LPS-responsive genes Il6, Il1β, Cox2 and iNos dose-dependently in concentrations of 1, 2, and 5 μM. At a concentration of 5 μM, GA significantly decreased Il6, Il1β, Cox2 and iNos RNA expression to 30% ($p < 0.05$), 39% ($p < 0.001$), 30% ($p < 0.05$) and 3% ($p < 0.05$), respectively (Fig. 2B–E, right column).

3.3. NE and GA differently affect the LPS-induced upregulation of iNos and Cox2 protein expression and secretion of respective signaling molecules

Further, we investigated the effect of NE and GA on post-translational expression of iNos and Cox2. In non-stimulated RAW264.7

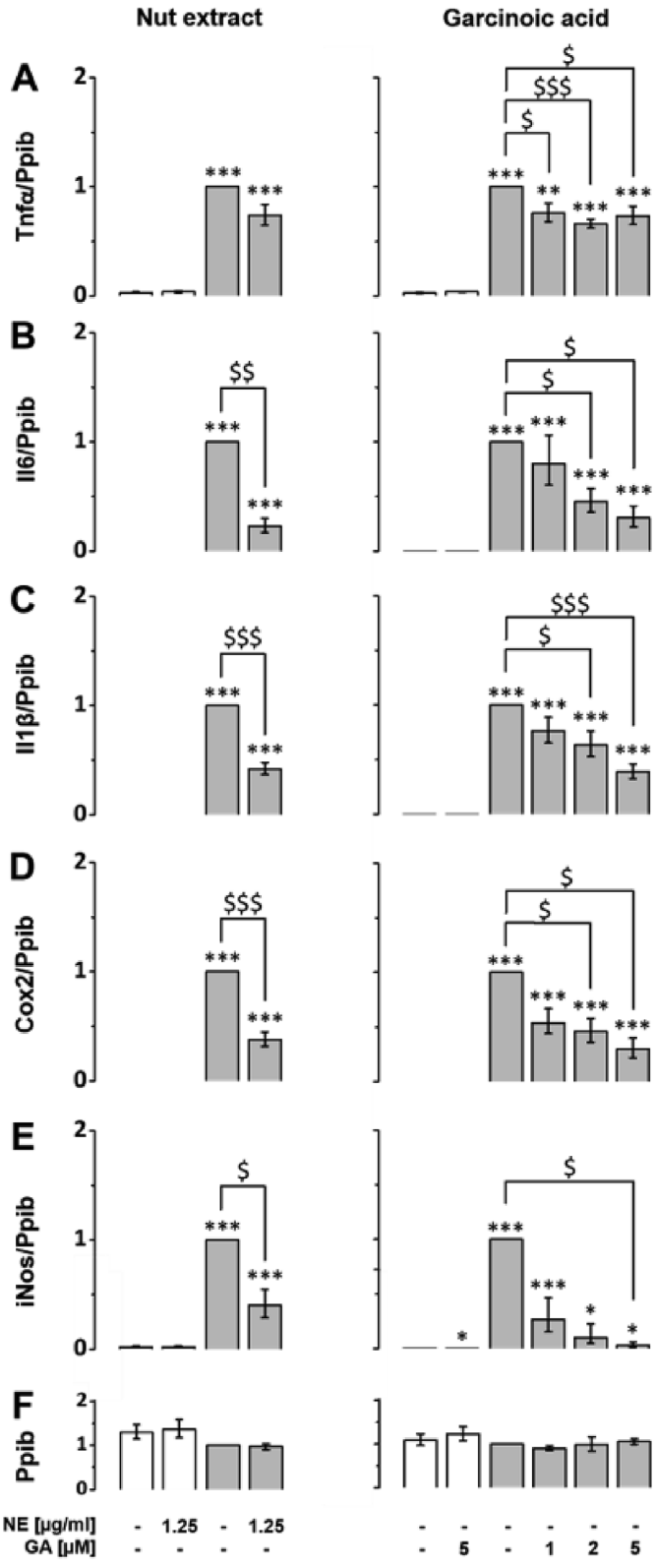

Fig. 2. Lipopolysaccharide-induced upregulation of Il6, Il1β, Cox2, iNos and Tnfα mRNA expression is blocked by the NE and isolated GA. RAW264.7 were pre-incubated with either NE (left column) GA (right column) or solvent (DMSO) for 24 h (white bars). For LPS-induced experiments, macrophages were co-incubated with 100 ng/ml LPS and either solvent, NE or GA at the doses indicated for another 24 h (grey bars). Samples co-cultured with solvent and LPS were defined as one. Expression levels of the inflammatory response genes **(A)** Tnfα, **(B)** Il6, **(C)** Il1β, **(D)** Cox2 and **(E)** iNos were measured using RT-qPCR and normalized to the mRNA expression of the reference gene **(F)** peptidylprolyl isomerase B (Ppib). Error bars display calculated minimum and maximum of SEM (SEM ± min, max) expression levels of four independent biological experiments, each measured in one or two technical replicates. *, $p < 0.05$; **$p < 0.01$; ***, $p < 0.001$ (*vs.* solvent control); $^{\$}$, $p < 0.05$; $^{\$\$}$, $p < 0.01$; $^{\$\$\$}$, $p < 0.001$ (*vs.* LPS treatment). Student's t-test was performed for statistical analysis.

macrophages, protein levels of iNos and Cox2 were neither detectable nor modulated by GA or NE. Treatment with NE and GA decreased LPS-induced protein expression of Cox2 to 62% ± 23% (left) and 67% ± 13% (right, $p < 0.0001$; Fig. 3A), respectively. The iNos protein expression was significantly diminished by NE (68% ± 10%, left) and GA (17% ± 11%, right, Fig. 3B, $p < 0.0001$) to a similar extent.

Since Cox2 and iNos expression regulate production and release of respective signaling molecules, the effect of NE and GA on the release of NO, TxB_2 and different prostanoids have been measured (Fig. 3C–E). While basal NO (Fig. 3C), TxB_2 (Fig. 3D) and prostaglandin (Fig. 3E, white bars) levels remained unchanged in the presence of NE and GA, treatment with LPS significantly elevates these signaling molecules in the supernatant of RAW264.7 macrophages ($p < 0.0001$, Fig. 3C–E). The LPS-induced production of NO was significantly decreased from 32.2 ± 3.7 µM (LPS control) to 26.0 ± 5.8 µM ($p < 0.05$) by NE and even more effectively by GA to 6.2 ± 5.7 µM ($p < 0.01$; Fig. 3C, grey bars). The release of TxB_2 was inhibited in LPS-activated macrophages by NE and GA to 37.3% ± 25.2% ($p < 0.01$) and 9.1% ± 7.8% ($p < 0.001$) remaining activity, respectively (Fig. 3D, grey bars). In addition, the effect of NE and GA on the release of different prostaglandins was measured by ultraperformance liquid chromatography-coupled tandem mass spectrometry (UPLC-MS/MS). Co-incubation of LPS and GA decreased the release of PGE_2 and PGD_2 (Fig. 3E) almost to baseline levels, 0.09 ± 0.03 RU ($p < 0.05$) and 0.05 ± 0.02 RU ($p < 0.01$), respectively, whereas NE decrease the prostaglandin levels to 0.53 ± 0.10 RU (PGE_2) and 0.49 ± 0.11 RU (PGD_2). To exclude that the potent inhibition of Cox-derived eicosanoids in LPS-activated macrophages depends on a direct inhibition of Cox isoenzymes, we determined the effect of GA on the activity of isolated bovine Cox1 and human recombinant COX2 in a cell-free assay. GA did not affect Cox1 and only weakly inhibited Cox2 (89 ± 13% residual activity) at a concentration of 10 µM (data not shown).

3.4. Local anti-inflammatory effects of GA in atherosclerotic lesions of aortic sinus

Based on the significant anti-inflammatory effects of GA shown here *in vitro*, we investigated its impact on the development of atherosclerotic plaques in male $ApoE^{-/-}$ mice fed with high fat diet (HFD). Under our experimental conditions body and organ weight (Suppl. Fig. S4A) as well as the plasma lipid profile (Suppl. Fig. S4B) of mice remained unchanged. Focusing on plaque morphology and stability, no significant differences were detected for morphological parameters including total lesion size, necrotic core area and lipid content analyzed using Hematoxylin and Eosin (H&E) and Oil Red O (ORO) staining, respectively. Collagen content (PSR), vascular cell adhesion protein (VCAM)-1 and cluster of differentiation (CD) 68, a marker for macrophage infiltration, remained unchanged (Fig. 4A). Analysis of intraplaque inflammatory profile revealed no change in monocyte chemoattractant protein (MCP)-1 and interleukin (IL)1β levels. However, treatment with GA significantly decreased nitrotyrosine level - a marker for inflammatory stress - in atherosclerotic plaques to 50% compared to the control group (Fig. 4B and Suppl. Fig. S2, $p < 0.05$).

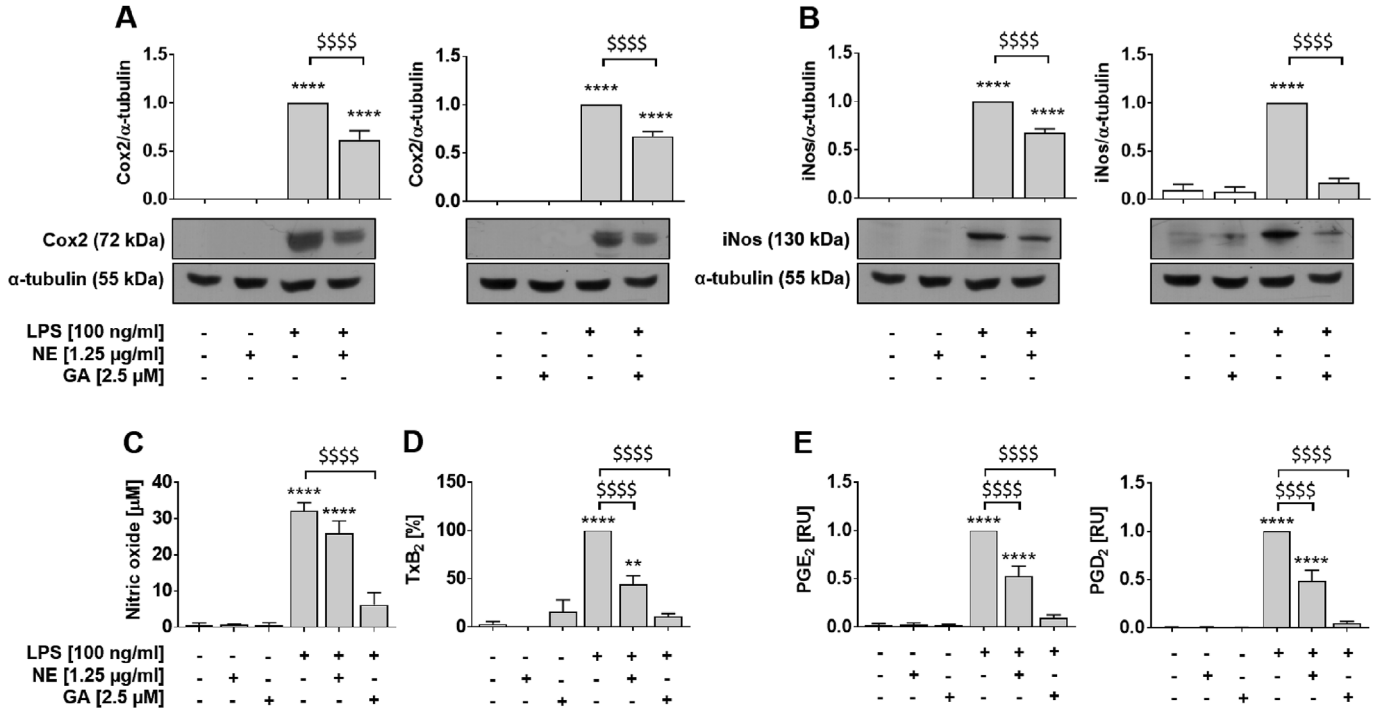

Fig. 3. Lipopolysaccharide-induced expression of iNos and Cox2 protein and secretion of respective signaling molecules are more potently blocked by GA compared to NE. RAW264.7 macrophages were incubated with either solvent (DMSO, white bars), NE or GA, or co-incubated with 100 ng/ml LPS (grey bars). The NE and GA decreased the protein expression of **(A)** Cox2 and **(B)** iNos after 24 h pre-incubation with NE or GA followed by 14 h and 24 h co-incubation with LPS, respectively. Samples incubated with LPS were defined as reference and were set as one. Protein levels were normalized to α-tubulin for quantification and representative Western blots are shown (for un-chopped versions see Suppl. Fig. S6). **(C)** Basal NO production, determined using Griess assay, were affected neither by the NE nor GA, whereas LPS-induced the formation of NO was significantly decreased by NE and even more effectively by purified GA. Treatment of RAW264.7 macrophages to measure released **(D)** TxB_2 and **(E)** PGs into culture supernatants followed the description in Fig. 2 except for use of 2.5 µM GA. Neither the NE nor GA altered the basal release of prostanoids. Treatment with LPS significantly induced TxB_2 and PG levels in the supernatant of macrophages and was set to 100% or one, respectively. Both, NE and GA decreased the release of TxB_2, PGE_2 and PGD_2 by LPS-activated macrophages Means of three independent biological experiments measured in two technical replicates **(A,B)**, three **(C)**, six **(D)** or four to five **(E)** independent biological experiments are shown; error bars display SEM. *, $p < 0.05$, **, $p < 0.01$, ***, $p < 0.001$ ****, $p < 0.0001$ (*vs.* control); $^{\$}$, $p < 0.05$, $^{\$\$}$, $p < 0.01$, $^{\$\$\$}$, $p < 0.001$, $^{\$\$\$\$}$, $p < 0.0001$ (*vs.* LPS treatment). Student's t-test and ANOVA followed by Tukey post-hoc tests with logarithmized values was performed for statistical analysis.

3.5. GA does not affect systemic levels of iNos and Cox signaling molecules

As shown in Fig. 3, GA significantly blocked Cox2 and iNos pathways in LPS-activated macrophages. To determine if these effects occur in our atherosclerotic mouse model, plasma levels of NO (Fig. 5A) and prostanoids (Fig. 5B–D) have been measured. Baseline prostanoid concentrations in plasma increased under atherosclerotic conditions 8-fold (TxB_2, $p > 0.01$), 1.4-fold (6 keto $PGF_{1\alpha}$, n.s.) and 8-fold (PGE_2, $p > 0.001$, Suppl. Fig. S5). However, treatment with GA did neither alter NO levels (Fig. 5A) nor changed prostanoid levels in mice (Fig. 5B–D).

3.6. GA differentially affects systemic and localized inflammation

Changes in the distribution of immune cells such as lymphocytes and monocytes and the modulation of their sub-populations play a pivotal role in atherosclerosis. Systemic (blood) and local (spleen) cell population have been changed after GA treatment in at least partly different extent. In blood, the total population of monocytes/macrophages as well as the pro-inflammatory $Ly6c^{high}$ and the anti-inflammatory $Ly6c^{low}$ monocyte sub-population remain unchanged (Fig. 6A). There is no change in B cell and CD8 T cell population. However, CD4 positive T cells are significantly downregulated in the GA-treated group by 14.8% ($p < 0.05$) and the CD4/CD8 ratio decreases from 2.1 ± 0.1 (control) to 1.9 ± 0.05 (GA treatment, $p = 0.077$). Further, natural killer (NK) and natural killer T (NKT) cells were significantly up-regulated 3.2% ± 0.4% vs. 5.6% ± 0.8%; 0.2% ± 0.02% vs. 0.6% ± 0.2%, respectively ($p < 0.05$, control vs. GA-treated group). In contrast, local (spleen) population of analyzed cell types remained unchanged, except for NK cells which were significantly upregulated (2.0% ± 0.1% vs. 2.8% ± 0.1%; $p < 0.001$, control vs. GA treatment).

4. Discussion and conclusions

Garcinia kola is known in Africa as a 'traditional' medicinal plant [7]. One of the significant phytochemicals found in *Garcinia kola* seeds is GA [7,18,19]. In order to obtain high yields of GA from *Garcinia kola* seeds, we developed an optimized extraction procedure for GA to ensure the most effective use of the seeds. Using our improved approach, we significantly increased the yield (6.6 fold) and purity (> 99%) of extracted GA (Fig. 1 and Suppl. Fig. S1). Extracted GA is purer than the commercially available product as well as the GA received using former protocols, consequently indicating that the *Garcinia kola* seeds were utilized optimally by our extraction method. Having reasonable amounts of pure GA accessible opens new application possibilities, such as (i) *in vitro* and *in vivo* studies as well as (ii) using GA as a starting product for the synthesis of the long-chain metabolites of vitamin E (LCMs) as described by Mazzini et al. [6] Synthesis of the LCMs is essential to study their physiological role, as the LCMs are not commercially available.

The bioactivity of the *Garcinia kola* plant has been studied *in vitro* as well as in animal and human studies, as recently reviewed [22]. Different studies demonstrated the radical scavenging, anti-oxidative and

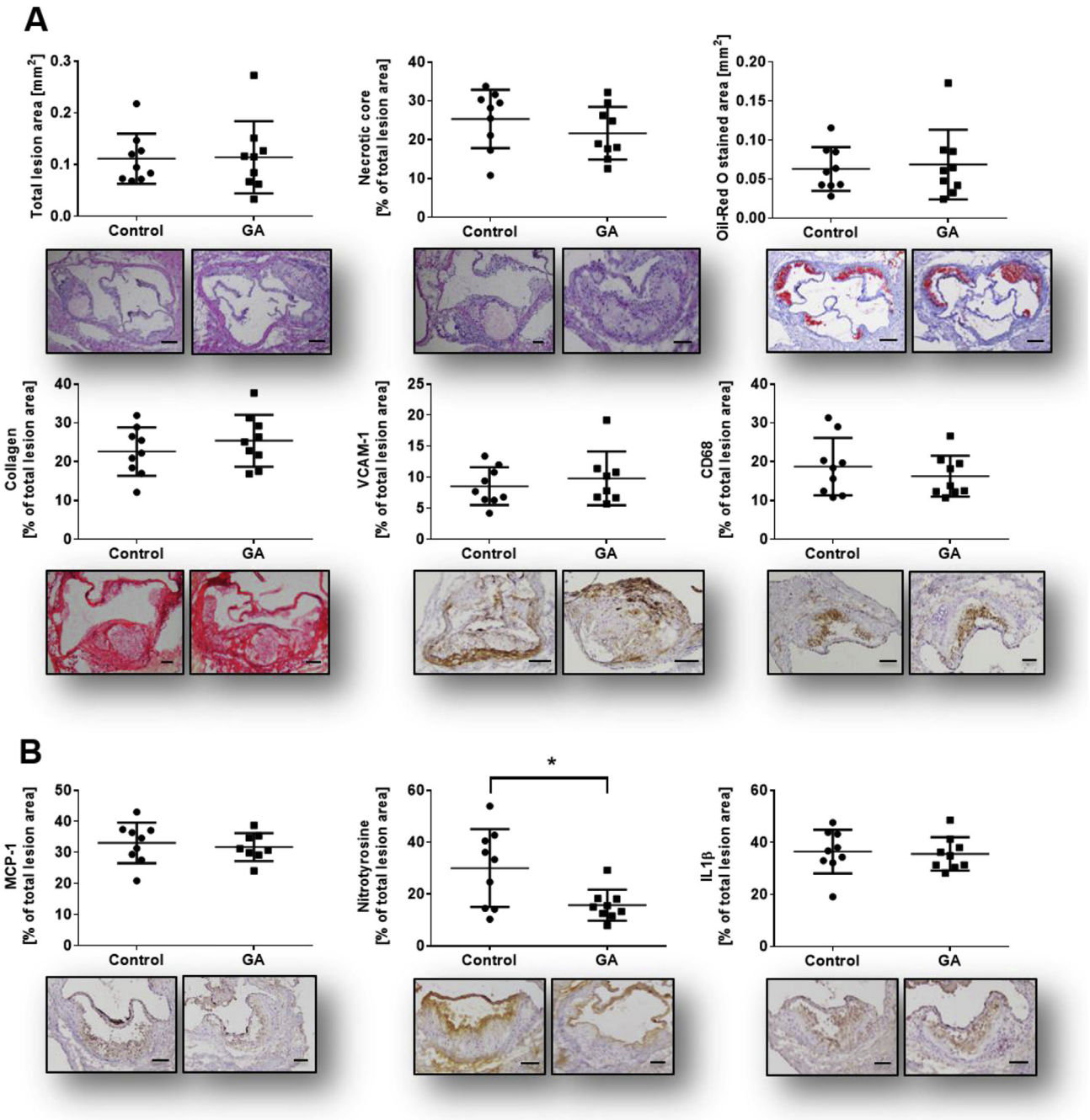

Fig. 4. Plaque morphology, stability and inflammatory profile of lesions. Frozen OCT embedded aortic sinus sections (6 μm) have been stained as follows: **(A)** Characterization of plaque morphology, stability and inflammation status has been analyzed using histological (Hematoxylin and Eosin; H&E, Oil Red O; ORO, Picro Sirus Red; PSR) and immunohistochemical staining (VCAM-1, CD68, MCP-1, nitrotyrosine, IL1β). No significant changes could be detected in all morphological parameters including total lesion size, necrotic core area (H&E), lipid content (ORO) and collagen content (PSR). GA application decreased inflammatory status as shown by a significant downregulation of nitrotyrosine level in the treatment group vs. control group. In contrast, adhesion marker (VCAM-1), macrophage content (CD68) and further inflammatory markers such as MCP-1 and IL1β remain unchanged. Single dots represent the mean of three to four sections per mouse. Error bars display calculated standard deviation. *, $p < 0.05$, scale bar 100 μm and 200 μm (total lesion size and ORO), magnification 100×. One-way ANOVA with multiple comparisons were calculated.

anti-inflammatory potential of the *Garcinia kola* plant, and the seeds in particular [3,7]. It has been shown that a methanol extract of the seeds reduces the LPS-induced NO production in the human macrophage cell line U937[3] and in rats [21], which is possibly mediated by one of its main phytochemicals, such as GA. Data on anti-inflammatory effects of isolated GA are rare. Until recently its anti-inflammatory potential was merely postulated based on its anti-oxidative effects [4]. To demonstrate the importance of GA for the reported anti-inflammatory effects of *Garcinia kola* seeds, we directly compared the effects of NE and GA *in vitro*. Our data revealed that both GA and NE interfere with anti-inflammatory signaling in LPS-stimulated RAW264.7 macrophages, with GA being slightly more efficient compared to NE (Figs. 2 and 3). Birringer et al. have shown that less than 1% of the *Garcinia kola* seeds is constituted by GA [18]. Since GA is soluble in organic solvents the percentage of GA in our NE is higher. Taking this into account, a significant contribution of GA to the anti-inflammatory effects of the NE is evident.

GA combines structural similarities of both, δ-T3 and the LCM of

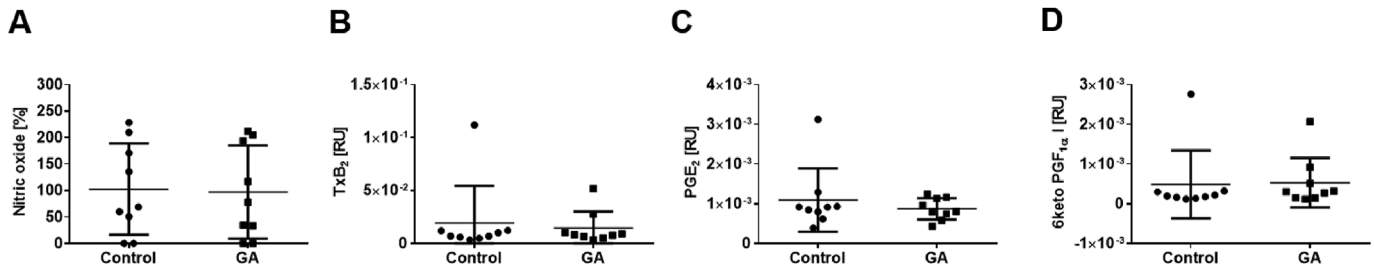

Fig. 5. GA does not affect systemic levels of iNos and Cox signaling molecules. Plasma samples from ApoE$^{-/-}$ mice fed with HFD and in parallel injected with GA or vehicle for eight weeks have been measured to determine **(A)** NO levels **(B)** thromboxane levels as well as **(C + D)** prostaglandin (PGE_2 and 6-keto $PGF_{1\alpha}$) levels. Mean of basal NO levels of vehicle control group was set as 100%. Treatment with GA did neither alter NO levels in mice (102.7% ± 28.8% vs. 97.1% ± 29.3%; control vs. treatment) nor the prostanoid levels (TxB_2: 1.939E-02 ± 1.162 E−02 vs. 1.443E-02 ± 0.523E-02, PGE_2: 1.092E-03 ± 0.2662 E−03 vs. 0.873E-03 ± 0.0908E-03, 6 keto $PGF_{1\alpha}$: 0.488E-03 ± 0.29 E−03 vs. 0.531E-03 ± 0.2088E-03; control vs. GA). Error bars display calculated SD. Student's t-test and ANOVA followed by Tukey post-hoc tests with logarithmized values was performed for statistical analysis.

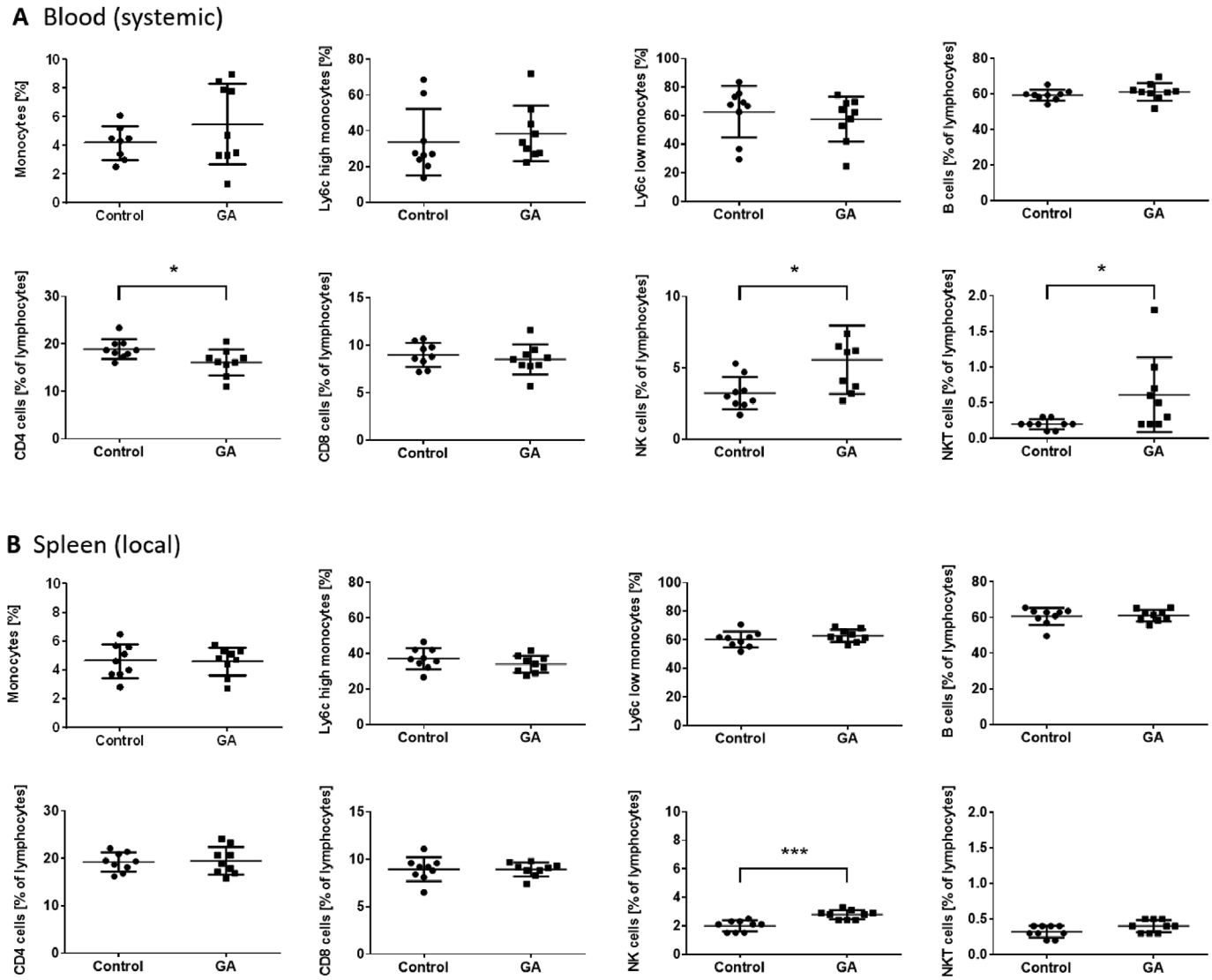

Fig. 6. GA modulates systemic and localized inflammation to different extent. Interactions of GA treatment with immune cell distribution were analyzed using flow cytometry. Systemic (blood) and local (spleen) cell population have been quantified using monocyte/macrophage, B cell and T cell specific fluorescent staining. **(A)** In blood total monocyte/macrophage population and sub-populations remained unchanged. There is no change in B cell and CD8 T cell population. CD4 positive T cells are significantly downregulated in GA-treated mice, 16.1% ± 0.9% compared to control group 18.9% ± 0.7%, whereas nature killer (NK) and natural killer T (NKT) cells were significantly upregulated 3.2% ± 0.4% vs. 5.6% ± 0.8%; 0.2% ± 0.02% vs. 0.6% ± 0.2%, respectively (control vs. GA-treated group). **(B)** In contrast local (spleen) population of tested cell types remained unchanged, except for an increase in NK cells (2.0% ± 0.1% vs. 2.8% ± 0.1%). Error bars display calculated SD. *, $p < 0.05$, ***, $p < 0.001$ (control vs. GA). Student's t-test was used.

vitamin E α-13′-COOH, with respect to the methylation pattern of the chromanol ring as well as the saturation and the terminal oxidation of the side chain, respectively. Within the group of vitamin E, δ-T3 is probably the most effective in inhibiting pro-inflammatory pathways [23]. For example, expression of Cox2, production of cytokines and release of PGE_2 and NO was inhibited in LPS-activated RAW264.7 macrophages by δ-T3 more effectively than by α-TOH, α-T3 and γ-T3 [9]. In line with these findings, Qureshi et al. have shown that Tnfα serum levels and expression of Il6, Il1β, iNos and Tnfα were effectively decreased by δ-T3 in LPS-stimulated peritoneal macrophages obtained from BALB/c mice [24]. Furthermore, GA (δ-TE-13'-COOH) has been described as the most potent 5-lipoxygenase (5-LO) inhibitor within the group of vitamin E metabolites [25].

α-13'-COOH is claimed to be a bioactive molecule since significant effects on lipid metabolism and homeostasis as well as inflammation have been reported [14,16,26,27]. In the study of Jiang and colleagues, the LCMs δ- and γ-13′-COOH were characterized as potent anti-inflammatory agents due to their ability to inhibit the COX2 pathway in IL1β-stimulated human lung adenocarcinoma A549 cells [14]. In addition, our group has recently shown that α-13′-COOH blocks the LPS-induced expression of inflammatory marker genes, proteins and related signaling molecules in LPS-stimulated RAW264.7 macrophages [16]. Similar anti-inflammatory properties have been recently discussed for the structurally related GA [28]. Here, we demonstrate that GA reduced the LPS-induced mRNA expression of iNos and other crucial inflammatory pathways (Fig. 2), followed by the inhibition of NO and other signaling molecules (Fig. 3C–E).

Based on the promising anti-inflammatory effects of GA *in vitro* and previous studies demonstrating anti-atherosclerotic effects of T3s[13], we tested the potential of GA as a treatment against the inflammation-driven disease atherosclerosis. For the *in vivo* application, a maximum dose of 1 mg/kg of GA was used; the dose of GA was chosen with respect to its low solubility in aqueous solutions and the need of using DMSO as solvent. We used the highest concentration of 0.8% DMSO that is allowed for long-term application in mice by the Animal Ethics Committee of the Alfred Medical Research and Education Precinct (AMREP), Melbourne, Australia. Due to the limited solubility of GA in aqueous solutions containing only 0.8% DMSO we had to limited the dose of GA to 1 mg/kg. Calculated to the total amount of blood (2 ml) in mice, with 1 mg/kg GA injected intraperitoneally, initial plasma concentrations of GA up to an equivalent of 35 μM could be achieved. We decided to use the highest possible dose of 1 mg/kg (35 μM) GA. However, we cannot exclude that the distribution and clearance of GA changes the actual concentration achievable *in vivo* and that higher concentrations are needed to achieve suitable concentrations *in vivo* resulting in anti-atherogenic properties of GA. We found a significant reduction of intra-plaque nitrotyrosine levels (Fig. 4B) – a marker for NO production as expected from our *in vitro* studies. Since elevated nitrotyrosine levels have been reported in human atherosclerotic lesions, its contribution to cardiovascular disease as a linking mechanism between inflammation and development of atherosclerosis has been discussed [29]. Other inflammatory marker, such as IL1β and MCP-1, remained unchanged in the plaque, although GA has been shown to block these pathways *in vitro* (Fig. 2C). The total plaque size was not affected by GA treatment, despite the apparent interference with local NO production. Overall, it can be assumed that the decrease of intra-plaque inflammation by GA was not sufficient to significantly impact the plaque size. As recently shown by Pein et al., GA potently inhibits 5-LO [25]. An association of the expression of 5-LO and the progression of atherosclerotic plaque formation [30], and more precisely plaque instability [31], in patients has been shown. However, there are discrepancies of 5-LO expression in atherosclerotic plaques of humans and mice. Whereas the expression of 5-LO is upregulated in carotid plaques in humans, there is no difference in the expression levels in wild-type mice (C57Bl/6) compared to atherosclerotic mice strains ($ApoE^{-/-}$ and $ApoE^{-/-}/LDLR^{-/-}$) fed a HFD [32]. Indeed, the $5\text{-}LO^{-/-}/ApoE^{-/-}$ knockout model or pharmacological inhibition of 5-LO in mice failed to show an impact on the progression of atherosclerosis [33]. Therefore, evidence for a contribution of 5-LO to the formation of atherosclerotic plaques is still on demand.

As shown in Fig. 3C–E, GA efficiently blocks the production of NO and prostanoids in LPS-activated macrophages *in vitro*. However, neither NO nor prostanoid levels are changed by GA in murine plasma samples. The atherosclerotic mouse model used in our study is characterized by a low-level chronic inflammation. Therefore, baseline NO and prostanoid plasma levels are at least 100-fold lower compared to levels in LPS-activated macrophages. The lack of excessive pre-activation could be a reason why we did not see inhibitory effects of GA on systemic pro-inflammatory signaling molecules in our study. Whether GA would be more effective in acute inflammation (e.g. sepsis), which is closer to our *in vitro* model, needs further investigation. We can also not exclude that a different treatment regime or animal model of atherosclerosis would lead to different results.

Monocytes play a pivotal role in atherogenesis. We found the total monocyte population and the $Ly6C^{low}$ and $Ly6C^{high}$ sup-populations in blood and spleen to be unchanged. Effects of α-TOH [34] and γ-T3[12] on monocyte and macrophage recruitment have been shown, respectively, but nothing was known for GA. In addition, we observed that lymphocyte populations, especially T cells, NKT and NK cells, are modulated under GA treatment. This demonstrates the importance of oxidative modifications of the side chain for vitamin E metabolites on regulatory effects. In blood, GA treatment decreased CD4 positive cells and the CD4/CD8 cell ratio without regulation the CD8 positive cell population. This finding goes in line with the earlier reported effects of vitamin E in Brown Norway rats [35] and chickens [36]. Further, NK and NKT cells, which are important for the defence against tumour cells, are significantly increased. Since these cells are known to regulate immune responses, their upregulation shows the involvement of GA on the immune system. In support, effects of α-TOH on increased NK cell activity and their tumorolytic activity in mice have been shown [37].

In summary, our improved procedure for the extraction of GA from *Garcinia kola* seeds enabled us to perform *in vitro* and *in vivo* investigations using pure GA. For the first time, we clearly demonstrate that both the NE and GA efficiently affect acute inflammation by inhibiting LPS-induced pro-inflammatory pathways *in vitro*. However, in atherosclerosis as a model of low level chronic inflammation this effect is not sufficient to make a significant difference in plaque size and plaque stability. Therefore, further studies are required to unravel the effects of GA in inflammation-driven diseases using different animal models to shed new light on the molecular modes of action of GA and to verify the *in vivo* importance of our findings.

Authors contribution

MW, JB, SK, LS, YCC, MZ, AS, AM, MS, MT, HP and AK performed the experiments. MW and SL designed the study. MW, MB, KP and SL supervised the project. MW wrote the manuscript. MW, JB, SK, LS, YCC, MZ, AS, AM, MS, AK, OW, MB, KP and SL carefully read and evaluated the manuscript and discussed the results.

Declarations of interest

None.

Sources and funding

The project was funded to SL by grants from Forschungskreis der Ernährungsindustrie (FEI) as part of an AiF (Arbeitsgemeinschaft industrieller Forschungsvereinigungen "Otto von Guericke") project of the Industrielle Gemeinschaftsforschung (IGF) and Thüringer Ministerium für Bildung, Wissenschaft und Kultur, Stiftung für Technologie und Forschung. Work of MW is supported by Deutsche

Forschungsgemeinschaft (DFG, Wa 3836/1-1). Work of SL and AK is also supported by the DFG (RTG1715) and work of SL additionally by the German Federal Ministry of Education and Research (nutriCARD, Grant agreement number 01EA1411A) and the Free State of Thuringia and the European Social Fund (2016 FGR 0045). The work of LS and OW is supported by the Free State of Thuringia and the European Social Fund (2016 FGR 0045), and OW and SL are funded by the DFG SFB 1278 Polytarget. AK was funded by the DFG (KO 4589/7-1). Garcinia kola seeds were a kind gift from AnalytiCon Discovery (Potsdam, Germany).

Acknowledgements

We thank Carsten Rohrer, Waltraud Scheiding and Inga Richter for their excellent technical assistance. Further, we acknowledge the assistance of Michelle Cinel for the Cobas measurements and Alex Bobik and Peter Kanellakis for providing the staining facility.

Appendix A. Supplementary data

Supplementary data to this article can be found online at https://doi.org/10.1016/j.redox.2019.101166.

References

[1] M.M. Iwu, A.R. Duncan, C.O. Okunji, New antimicrobials of plant origin, Am. Soc. Hortic. Sci. Press (1999) 457–462.
[2] R.A. Hussain, A.G. Owegby, P. Parimoo, P. G. Kolanone Waterman, A novel polyisoprenylated benzophenone with antimicrobial properties from the fruit of Garcinia kola, Planta Med. 44 (1982) 78–81.
[3] T. Okoko, In vitro antioxidant and free radical scavenging activities of Garcinia kola seeds, Food Chem. Toxicol. Int. J. Publ. Br. Ind. Biol. Res. Assoc. 47 (2009) 2620–2623.
[4] K. Terashima, Y. Takaya, M. Niwa, Powerful antioxidative agents based on garcinoic acid from Garcinia kola, Bioorg. Med. Chem. 10 (2002) 1619–1625.
[5] M.K. Tchimene, et al., Bio-flavonoids and garcinoic acid from Garcinia kola seeds with promising local anesthetic potentials, Int. J. Pharmacogn. Phytochem. Res. 7 (2015) 764–767.
[6] F. Mazzini, M. Betti, T. Netscher, F. Galli, P. Salvadori, Configuration of the vitamin E analogue garcinoic acid extracted from Garcinia Kola seeds, Chirality 21 (2009) 519–524.
[7] A.O. Adesuyi, I.K. Elumm, F.B. Adaramola, A.G.M. Nwokocha, Nutritional and phytochemical screening of Garcinia kola, Adv. J. Food Sci. Technol. 4 (2012) 9–14.
[8] L.-T. Ng, H.-J. Ko, Comparative effects of tocotrienol-rich fraction, α-tocopherol and α-tocopheryl acetate on inflammatory mediators and nuclear factor kappa B expression in mouse peritoneal macrophages, Food Chem. 134 (2012) 920–925.
[9] M.-L. Yam, S.R. Abdul Hafid, H.-M. Cheng, K. Nesaretnam, Tocotrienols suppress proinflammatory markers and cyclooxygenase-2 expression in RAW264.7 macrophages, Lipids 44 (2009) 787–797.
[10] L. Allen, et al., Effects of delta-tocotrienol on obesity-related adipocyte hypertrophy, inflammation and hepatic steatosis in high-fat-fed mice, J. Nutr. Biochem. 48 (2017) 128–137.
[11] A.A. Qureshi, et al., Inhibition of nitric oxide in LPS-stimulated macrophages of young and senescent mice by δ-tocotrienol and quercetin, Lipids Health Dis. 10 (2011) 239.
[12] L. Zhao, et al., Gamma-tocotrienol attenuates high-fat diet-induced obesity and insulin resistance by inhibiting adipose inflammation and M1 macrophage recruitment, Int. J. Obes. 39 (2005) 438–446 (2015).
[13] A. Shibata, et al., High purity tocotrienols attenuate atherosclerotic lesion formation in apoE-KO mice, J. Nutr. Biochem. 48 (2017) 44–50.
[14] Q. Jiang, et al., Long-chain carboxychromanols, metabolites of vitamin E, are potent inhibitors of cyclooxygenases, Proc. Natl. Acad. Sci. U. S. A. 105 (2008) 20464–20469.
[15] L. Schmölz, et al., Structure-Function relationship studies in vitro reveal distinct and specific effects of long-chain metabolites of vitamin E, Mol. Nutr. Food Res. 61 (2017).
[16] M. Wallert, et al., α-Tocopherol long-chain metabolite α-13'-COOH affects the inflammatory response of lipopolysaccharide-activated murine RAW264.7 macrophages, Mol. Nutr. Food Res. 59 (2015) 1524–1534.
[17] K. Alsabil, et al., Semisynthetic and natural garcinoic acid isoforms as new mPGES-1 inhibitors, Planta Med. 82 (2016) 1110–1116.
[18] M. Birringer, et al., Proapoptotic effects of long-chain vitamin E metabolites in HepG2 cells are mediated by oxidative stress, Free Radic. Biol. Med. 49 (2010) 1315–1322.
[19] K. Terashima, et al., Constituents of the seeds of garcinia kola: two new antioxidants, garcinoic acid and garcinal, Heterocycles 45 (1997) 1559–1566.
[20] E.G. Bligh, W.J. Dyer, A rapid method of total lipid extraction and purification, Can. J. Biochem. Physiol. 37 (1959) 911–917.
[21] T. Okoko, S. Ndoni, The effect of Garcinia kola extract on lipopolysaccha-ride-induced tissue damage in rats, Trop. J. Pharmaceut. Res. 8 (2009) 27–31.
[22] S. Kluge, et al., Garcinoic acid: a promising bioactive natural product for better understanding the physiological functions od tocopherol metabolites, Studies in Natural Products Chemistry, vol. 51, 2016, pp. 435–481.
[23] B.B. Aggarwal, C. Sundaram, S. Prasad, R. Tocotrienols Kannappan, the vitamin E of the 21st century: its potential against cancer and other chronic diseases, Biochem. Pharmacol. 80 (2010) 1613–1631.
[24] A.A. Qureshi, J.C. Reis, C.J. Papasian, D.C. Morrison, N. Qureshi, Tocotrienols inhibit lipopolysaccharide-induced pro-inflammatory cytokines in macrophages of female mice, Lipids Health Dis. 9 (2010) 143.
[25] H. Pein, et al., Endogenous metabolites of vitamin E limit inflammation by targeting 5-lipoxygenase, Nat. Commun. 9 (2018).
[26] S. Ciffolilli, et al., Human serum determination and in vitro anti-inflammatory activity of the vitamin E metabolite α-(13'-hydroxy)-6-hydroxychroman, Free Radic. Biol. Med. 89 (2015) 952–962.
[27] M. Wallert, et al., Long-chain metabolites of α-tocopherol occur in human serum and inhibit macrophage foam cell formation in vitro, Free Radic. Biol. Med. 68 (2014) 43–51.
[28] L. Schmölz, et al., Regulation of inflammatory pathways by an a-tocopherol long-chain metabolite and a d-tocotrienol-related natural compound, Free Radic. Biol. Med. 75 (Suppl 1) (2014) S48.
[29] M.H. Shishehbor, et al., Association of nitrotyrosine levels with cardiovascular disease and modulation by statin therapy, JAMA 289 (2003) 1675–1680.
[30] S. Matsumoto, et al., Effect of treatment with 5-lipoxygenase inhibitor VIA-2291 (atreleuton) on coronary plaque progression: a serial CT angiography study: 5-Lipoxygenase inhibitor and coronary plaque, Clin. Cardiol. 40 (2017) 210–215.
[31] F. Cipollone, et al., Association between 5-lipoxygenase expression and plaque instability in humans, Arterioscler. Thromb. Vasc. Biol. 25 (2005) 1665–1670.
[32] H. Qiu, et al., Expression of 5-lipoxygenase and leukotriene A4 hydrolase in human atherosclerotic lesions correlates with symptoms of plaque instability, Proc. Natl. Acad. Sci. U. S. A. 103 (2006) 8161–8166.
[33] R.Y. Cao, T. St. Amand, R. Gräbner, A.J.R. Habenicht, C.D. Funk, Genetic and pharmacological inhibition of the 5-lipoxygenase/leukotriene pathway in atherosclerotic lesion development in ApoE deficient mice, Atherosclerosis 203 (2009) 395–400.
[34] F. Marra, et al., Expression of monocyte chemotactic protein-1 precedes monocyte recruitment in a rat model of acute liver injury, and is modulated by vitamin E, J. Investig. Med. Off. Publ. Am. Fed. Clin. Res. 47 (1999) 66–75.
[35] J.Y. Gu, et al., Dietary effect of tocopherols and tocotrienols on the immune function of spleen and mesenteric lymph node lymphocytes in Brown Norway rats, Biosci. Biotechnol. Biochem. 63 (1999) 1697–1702.
[36] G.F. Erf, W.G. Bottje, T.K. Bersi, M.D. Headrick, C.A. Fritts, Effects of dietary vitamin E on the immune system in broilers: altered proportions of CD4 T cells in the thymus and spleen, Poultry Sci. 77 (1998) 529–537.
[37] M.K. Ashfaq, H.S. Zuberi, M. Anwar Waqar, Vitamin E and beta-carotene affect natural killer cell function, Int. J. Food Sci. Nutr. 51 (Suppl) (2000) S13–S20.